ELEMENTA
Science of the Anthropocene

Mao, J, et al. 2021. Comparative study of chemical characterization and source apportionment of $PM_{2.5}$ in South China by filter-based and single particle analysis. *Elem Sci Anth*, 9: 1. DOI: https://doi.org/10.1525/elementa.2021.00046

RESEARCH ARTICLE

Comparative study of chemical characterization and source apportionment of $PM_{2.5}$ in South China by filter-based and single particle analysis

Jingying Mao[1,2], Liming Yang[3], Zhaoyu Mo[4], Zongkai Jiang[5], Padmaja Krishnan[6], Sayantan Sarkar[7], Qi Zhang[8], Weihua Chen[1,2], Buqing Zhong[1,2], Yuan Yang[10], Shiguo Jia[8,9,*], and Xuemei Wang[1,2,*]

Single particle aerosol mass spectrometers (SPAMS) have created significant interest among atmospheric scientists by virtue of their ability to provide real-time size-resolved information on the chemical composition of aerosols. The objective of this study is to evaluate the newly developed single particle analysis technique in terms of chemical characterization and source apportionment of ambient aerosols by comparing it with traditional filter-based methods. In this study, an air quality monitoring campaign was conducted over a period of 25 days at an urban area in Yulin city, southern China, by employing both SPAMS and traditional filter-based measurements to establish the performance of SPAMS. It was observed that the chemical characterization of particles based on SPAMS did not agree well with the filter-based analysis. Based on the filter analysis, sulfate was the most abundant component in $PM_{2.5}$ (23.5%), followed by OC (18.1%), while for single particle analysis (number concentration), EC-containing particles showed the largest contribution to $PM_{2.5}$ (>40%), followed by OC (15.7%). In terms of source apportionment via positive matrix factorization, six sources were identified by each of the two approaches. Both the approaches showed relatively good agreements for secondary species, traffic, and dust sources; however, discrepancies were noted for industry, fossil fuel, and biomass burning sources. Finally, investigation of diurnal profiles and two specific emission episodes monitored during the Chinese New Year and traffic activities demonstrated the relative advantage of single particle analysis over filter-based methods. Overall, single particle analysis can provide source apportionment with a high time resolution, which is helpful for policy makers to analyze and implement emergency control strategies during air pollution episodes. However, SPAMS performs quantification of number concentration rather than mass concentration and is limited to particles larger than 200 nm, which leads to discrepancies between the two methods. SPAMS measurements can therefore not simply replace traditional filter-based analyses, which needs to be carefully considered in the selection of the monitoring implementation.

Keywords: Air quality, Source apportionment, Single particle, Real-time measurement, Pollution control

[1] Institute for Environmental and Climate Research, Jinan University, Guangzhou, P.R. China
[2] Guangdong-Hongkong-Macau Joint Laboratory of Collaborative Innovation for Environmental Quality, Guangzhou, China
[3] Department of Chemical and Bimolecular Engineering, National University of Singapore, Singapore
[4] Scientific Research Academy of Guangxi Environmental Protection, Nanning, China
[5] College of Earth Science and Engineering, Shandong University of Science and Technology, Qingdao, P.R. China
[6] Department of Civil Engineering, National University of Singapore, Singapore
[7] School of Engineering, Indian Institute of Technology (IIT) Mandi, Kamand, Himachal Pradesh, India
[8] School of Atmospheric Sciences, & Guangdong Province Key Laboratory for Climate Change and Natural Disaster Studies, Sun Yat-sen University, Guangzhou, P. R. China
[9] Southern Laboratory of Ocean Science and Engineering (Guangdong, Zhuhai), Zhuhai, P.R. China
[10] State key laboratory of Atmospheric Boundary Layer Physics and Atmospheric Chemistry (LAPC), Institute of Atmospheric Physics, Chinese Academy of Sciences, Beijing, China

* Corresponding authors:
Emails: eciwxm@jnu.edu.cn; jiashg3@mail.sysu.edu.cn

1. Introduction

China has faced a severe air pollution challenge in recent years due to its fast-developing economy and large-scale urbanization. Several studies have established $PM_{2.5}$ (particles with aerodynamic diameter smaller than 2.5 μm) as the major air pollutant in China, responsible for significant health impacts and economic losses (Bai et al., 2018; Xie et al., 2019). A city-level study has revealed that $PM_{2.5}$-related deaths in China could range from 0.77 million to 1.258 million depending on the nature of exposure-response functions in 2016 (Maji et al., 2018). This is not surprising given that $PM_{2.5}$ is classified as the world's largest environmental health risk, contributing to approximately 7 million deaths per year worldwide, especially in the Western Pacific and Southeast Asia (European Environment Agency, 2015; World Health Organization, 2014).

Owing to a significant reduction in visibility and increased threat to public health, the Chinese government has implemented several emission reduction strategies in the recent years. Annual concentration reduction targets for $PM_{2.5}$ were set for the most economically developed regions of China to substantially curtail their $PM_{2.5}$ levels by 2017 as compared to 2013 values. For example, reduction targets of 25%, 20%, and 15% were proposed for the Beijing–Tianjin–Hebei region in northern China, Yangtze River Delta in eastern China, and the Pearl River Delta in southern China, respectively (State Council of PRC, 2013). A robust understanding of the major sources of $PM_{2.5}$ is vital to implement effective emission reduction strategies and regulations. Currently, source apportionment is the primary tool used by the Chinese government to identify and quantify the major sources of fine particles. Positive matrix factorization (PMF) has been widely adopted over the past few decades as an effective approach to identify the sources of air pollution and quantitatively estimate the pollutant levels contributed by various sources through statistical interpretation of ambient measurements (Paatero and Tapper, 1994).

Most source apportionment studies in China and elsewhere are typically carried out based on chemical analysis of particulate matter collected on filters. For example, using PMF based on filter measurements, Zong et al. (2016) identified the major sources of $PM_{2.5}$ in North China as fossil fuel combustion (29.6%), biomass burning (19.3%), and vehicle emission (15.9%). Employing a wet denuder-steam jet aerosol collector system, Guo et al., (2010) analyzed size-resolved aerosol particles and observed that regional secondary aerosol formation could lead to aerosol pollution during summer in Beijing, which accounted for more than 50% of fine particle mass. Studies such as these that utilize the traditional offline measurement technique involving collection of particles on filters followed by chemical processing are susceptible to biases originating from the potential decay or degeneration of chemical species during preservation, transportation, and sample analysis. To overcome these challenges, high time resolution analytical techniques have been recently developed to characterize short-term variability in aerosol concentrations and to isolate individual sources (Prather et al., 2008; Zhang et al., 2018; Zhang et al., 2018; Wang et al., 2019). Despite potential issues of bias, as discussed before, filter-based analysis still remains the most widely used approach worldwide and is considered as the benchmark (e.g., United States and China). Therefore, it is vital that the newly developed single particle method is compared and validated against the traditional filter-based analysis to establish the efficacy of the single particle method and identify potential discrepancies.

The single particle aerosol mass spectrometer (SPAMS) offers real-time detection of atmospheric particles and can simultaneously provide information on the size distribution, number concentration, and chemical composition of the particles at a single particle level. This information can be collated to a direct source apportionment based on single particle number concentration and chemical composition (Kelly et al., 2003). Only a limited number of studies thus far have verified high-resolution online measurements against the traditional offline analysis; for example, Huang et al., (2014) compared major ions (sulfate, nitrate, and ammonium) measured in filter samples against those measured online by a monitor for aerosols and gases in ambient air (MARGA) system, and the two sets of data showed agreement within 25%. However, verification of SPAMS data and its interpretation by comparison with offline filter-based measurements have seldom been reported.

In view of this knowledge gap, the main objective of this study was to compare the source apportionment of $PM_{2.5}$ based on single particle and traditional filter-based analyses. To this end, we conducted an air quality monitoring campaign for a period of 25 days at an urban area in Yulin city, southern China, by employing both SPAMS (corresponding to particle number concentration) and traditional filter-based collection and analysis (corresponding to particle mass concentration). The mass and number concentration data from this campaign were then input to the PMF model in order to determine the emission sources of aerosols. Additionally, the high time resolution measurements from SPAMS were harnessed to analyze diurnal variation and episodic pollution events which cannot be captured by the filter-based analysis.

2. Experimental

2.1. Sampling location and period

This campaign was carried out at Yulin Environmental Monitoring Center (20 m above the ground), Guangxi, China (N22°38′28.65″, E110°10′1.70″), as depicted in **Figure 1**. Two bus interchanges were located at approximately 500 m northeast and 900 m north from the sampling site, respectively. $PM_{2.5}$ samples were collected daily from 6:30 AM to 6:00 PM (daytime) and from 6:30 PM to 6:00 AM (nighttime) during February 25 (6:30 PM)–March 22 (6:00 PM), 2016. A total of 49 filter samples were collected and processed while three samples were lost due to contamination. Single particle analysis was simultaneously conducted from February 25 (6:00 PM)–March 22 (11:00 PM), 2016. A total of 596 h of samples were collected and processed, while samples for 34 h could not be obtained due to contamination or malfunctioning of the instrument.

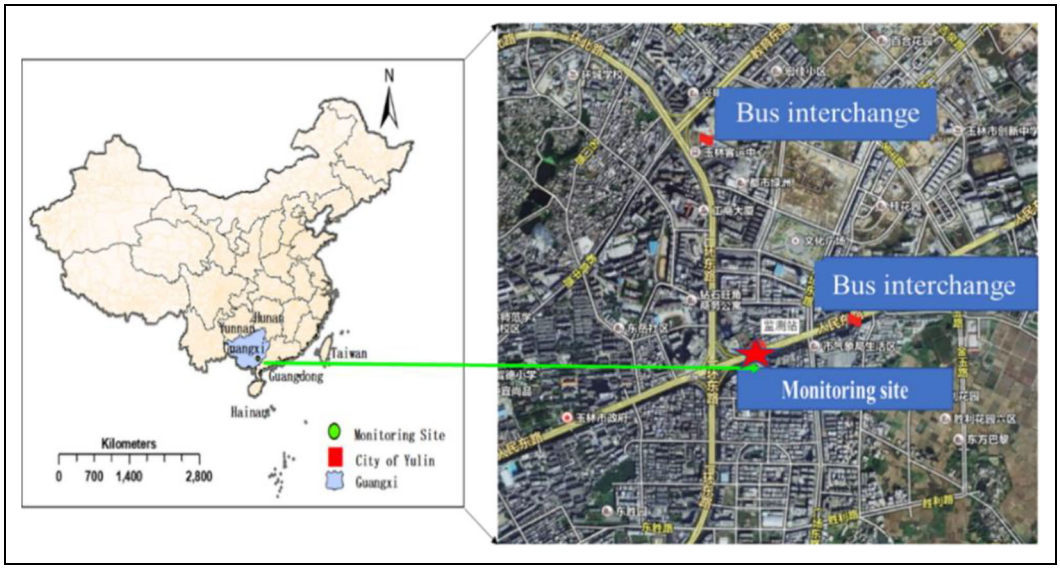

Figure 1. Sampling location in Yulin, China, indicated with a star. DOI: https://doi.org/10.1525/elementa.2021.00046.f1

2.2. Instrumentation and chemical analysis

2.2.1. $PM_{2.5}$ sample collection

$PM_{2.5}$ aerosol samples were collected on Pallflex Tissue quartz membrane filters (90 mm diameter, Whatman) using a TH150D III sampler (Wuhan Tianhong Environmental Protection Industry Co., Ltd., Wuhan, China) with a flow rate of 100 L min^{-1}. Quartz membrane filters were preheated in a muffle furnace at 450 °C for 4 h to remove residual carbon before usage. The filters were conditioned in a desiccator for 48 h before and after sampling and gravimetric weighing was carried out using a microbalance (BT224S, *Sartorius*) in a controlled environmental chamber at a temperature of 25 °C and relative humidity less than 38%. The collected filter samples were wrapped in organic-free aluminum foil (baked overnight) and stored in a freezer (–25 °C) before analysis. The aerosol-laden filters were then cut into different pieces for the quantification of metal species, water-soluble ionic species, and carbonaceous species.

2.2.2. Chemical analysis of $PM_{2.5}$ particles

For metal species analysis, half of the filter was transferred into Teflon tubes with a 10-mL mixture of acid solution. Each 1000 mL of the acid solution was prepared with 167.5 mL of 65% HNO_3 (Merck, for analysis EMSURE ISO), 55.5 mL of 37% HCl (Merck, for analysis EMSURE ISO), and 777 mL of ultrapure water according to the Chinese Technical Specification for Aerosol Environmental Monitoring (HJ777-2015). The filter sample in the acid solution was microwaved at 200 °C for 20 min under an operating power of 600 W, which was followed by the quantification of 18 metals (Al, Fe, Ca, Mg, Ti, K, Na, V, Cr, Hg, Mn, Ni, Cu, Zn, As, Cd, Pb, and Ba) via an inductively coupled plasma mass spectrometry system (ICAP-Q, Thermo Scientific, Waltham, MA, USA). Standard solution was spiked on blank filters to track recovery of each element for each batch. The standard filters underwent the same analytical procedure as the aerosol-laden filters, and recoveries were in the range of 85%–115% for all the metals.

For quantification of ionic species, a portion of the filter underwent water extraction in an ultrasonic bath for 30 min. An aliquot of the water extract was then analyzed by ion chromatography (Dionex, ICS-1000) for anionic and cationic species including fluoride (F^-), chloride (Cl^-), magnesium (Mg^{2+}), nitrate (NO_3^-), ammonium (NH_4^+), and sulphate (SO_4^{2-}). Potassium (K^+), calcium (Ca^{2+}), and sodium (Na^+) were not included since these elements had been measured using ICP-MS.

Carbonaceous compounds including organic carbon (OC) and elemental carbon (EC) were quantified using a thermal/optical carbon analyzer (DRI Model 2015, Atmoslytic Inc., Reno, NV, USA). Briefly, following the IMPROVE thermal/optical reflectance protocol (Chow et al., 1993; Baldauf et al., 2002; Kochy et al., 2002), a 0.495 cm^2 punch of filter was analyzed for eight carbon fractions. OC fractions OC1, OC2, OC3, and OC4 were liberated under a nonoxidizing He atmosphere at lower temperatures up to 580 °C, while EC comprising of EC1, EC2, and EC3 was combusted in an oxidizing atmosphere with 98% He and 2% O_2 at temperatures up to 840 °C. The liberated carbon was oxidized to carbon dioxide (CO_2) by heated manganese dioxide (MnO_2), which was then quantified by a nondispersive infrared detector to obtain the corresponding OC and EC. The sample results were corrected using the average concentration of the field blank filters ($n = 4$).

2.2.3. SPAMS analysis

The SPAMS (Hexin Analytical Instrument Co., Ltd., Guangzhou, China) is an instrument designed to measure real-time particle size distribution and chemical composition of aerosols. A more detailed description on its operation can be found elsewhere (Li et al., 2011). Briefly, ambient particles were introduced into the SPAMS through a 2–100 μm metal orifice into the vacuum system, following

which the polydisperse particles were focused onto a centerline by an aerodynamic lens. After leaving the aerodynamic lens, the single particles were introduced into the diameter sizing region. Based on the transit time of single particles, two continuous 532 nm lasers were employed to size the particles. Finally, the sized particles reached the laser desorption/ionization region, and both positive and negative ions were generated by a 266 nm Nd: YAG laser, which were then analyzed by a bipolar mass spectrometer analyzer. The mass spectra data obtained by SPAMS was loaded into a Matlab-based toolkit called Yet Another ATOFMS Data Analyzer (2008), and the toolkit was used to search particular mass spectral features (Allen, 2001; Lie et al., 2016). The mass-to-charge (m/z) ratio of characteristic ions used to identify different species is listed in Table S3.

2.3. Source apportionment

Source contributions for both particle number and mass concentrations were estimated by the U.S. Environmental Protection Agency's Positive Matrix Factorization tool (U.S. EPA, PMF), a bilinear unmixing model that identifies factors that serve to approximately reconstruct the measured mass concentration (Ulbrich et al., 2009). Each factor was comprised of a constant mass spectrum and a time series of mass concentration, and all values in the factors were constrained to be positive. By minimizing the sum of the weighed squared residuals of the fit (known as Q), the PMF model was solved with the EPA PMF 5.0 using the high-resolution mass spectral matrix of all species and associated error matrix as inputs (Paatero and Tapper, 1994). It is worthwhile to mention that for number concentration, only the ions with detection ratios larger than 0.5% (40 ions in total) were considered as true data and used for data analysis. Furthermore, the number concentration averaged over 1 h was used as input. For mass concentration, a total of 26 species (18 metals, 6 ions, and 2 carbonaceous compounds) were used as input. However, the concentration of Ni, Cr, Hg, F^-, and Mg^{2+} were excluded from the PMF analysis due to their low signal to noise ratio (see S1 and S2 in Supplementary Information). The uncertainty for each filter sample was estimated using the method by Tan et al. (2014) as per Equations 1 and 2. Other detailed information including categorizations of variables and selection of the number of factors can be found in Sections S1 and S2 in the Supplementary Information.

$$U = 2 \times \mathrm{MDL}(c \le \mathrm{MDL}). \quad (1)$$

$$U = \sqrt{(P \times c)^2 + (\mathrm{MDL})^2}(c > \mathrm{MDL}). \quad (2)$$

Where U is the overall uncertainty; P is the measurement uncertainty, which is expressed as a percentage of concentration (10%); c is the concentration of the sample; MDL is the method detection limit. For SPAMS analysis, a 20% uncertainty (U) was assumed as suggested by Zhou et al. (2016).

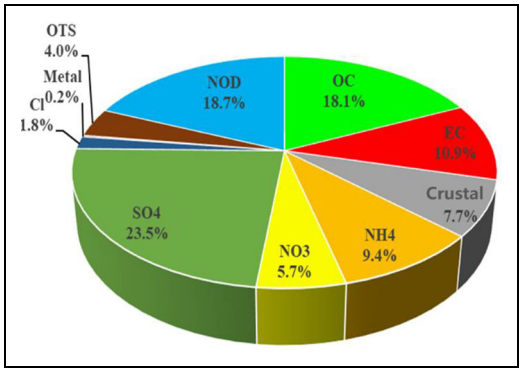

Figure 2. The reconstructed chemical map for $PM_{2.5}$ based on mass concentration during the study period, including SO_4^{2-}, NO_3^-, NH_4^+, Cl^-, crustal, EC, OC, metal, other soluble ions (OTS), and undetected fraction (NOD). DOI: https://doi.org/10.1525/elementa.2021.00046.f2

3. Results and discussion

3.1. Characteristics of $PM_{2.5}$

Figure 2 represents the detailed aerosol chemical composition of $PM_{2.5}$ based on particle mass concentration. The averaged $PM_{2.5}$ concentration for the entire measurement period was 41.9 ± 15.9 μg m^{-3}. Sulfate, likely originating from the oxidation of the gaseous precursor SO_2, was the most abundant component of $PM_{2.5}$ (9.7 ± 4.8 μg m^{-3}, 23.5%), with the ratio of sulfate to total $PM_{2.5}$ being similar to those reported from other megacities such as Guangzhou (Tao et al., 2012; Tao et al., 2017). OC, which is emitted from fossil fuel combustion and biomass burning, or produced in the atmosphere from photochemical reactions of volatile organic compounds (VOCs; Song et al., 2006), was the second largest component of $PM_{2.5}$ (8.0 ± 4.5 μg m^{-3}, 18.1%). EC, which is usually emitted from carbon fuel-based combustion processes and is exclusively associated with primary emissions such as vehicles (Wu and Yu, 2016; Mao et al., 2018), was the third largest component of $PM_{2.5}$ (5.1 ± 4.2 μg m^{-3}) contributing 10.9% to $PM_{2.5}$ mass. The two secondary inorganic species, nitrate and ammonium together, contributed 15.1% to total $PM_{2.5}$, while crustal material, potentially from road dust (Upadhyay et al., 2015), contributed 7.7%.

A total of 2,474,981 particles were sized, and 397,311 particles (the average hit rate was 16.1%) with both positive and negative ion mass spectra were analyzed via SPAMS during the study period. **Figure 3** shows the temporal trends of particle number concentration measured using SPAMS and particle mass concentration from filter-based measurements. The temporal trend of particle number and mass concentrations showed a reasonable agreement during the study period with a correlation coefficient (R) of 0.69 ($P < 0.05$).

On the other hand, the chemical profile of particles based on SPAMS data was significantly different from that obtained using the filter measurements. As shown in the plot of $PM_{2.5}$ composition based on number concentration (**Figure 4**), EC-containing particles had the largest contribution to $PM_{2.5}$ (>40%), followed by OC-containing particles (15.7%). Levoglucosan-containing particles and

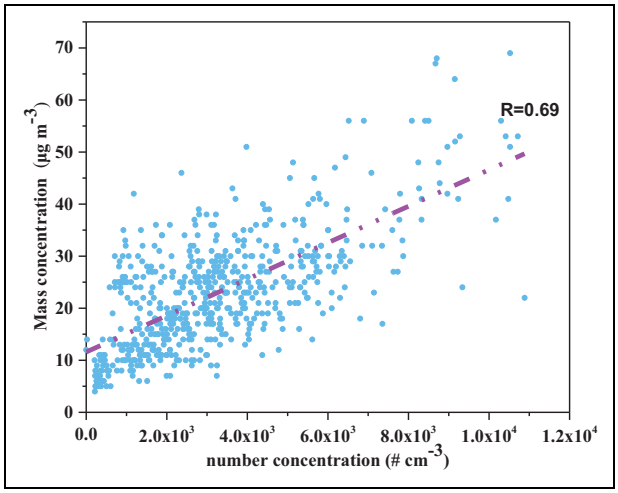

Figure 3. Scatterplot of mass and number concentration of $PM_{2.5}$. DOI: https://doi.org/10.1525/elementa.2021.00046.f3

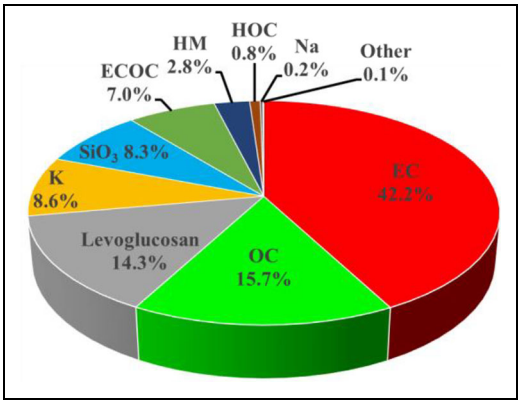

Figure 4. The reconstructed chemical map for $PM_{2.5}$ based on number concentration during the study period, including EC (elemental carbon-containing particles), OC (organic carbon-containing particles), Levoglucosan (Levoglucosan-containing particles), K (K^+-containing particles), Na (Na^+-containing particles), SiO_3 (SiO_3^- containing particles), ECOC (EC and OC combined particles), HM (heavy metal-containing particles), HOC (high molecular OC), and other undetected fractions. DOI: https://doi.org/10.1525/elementa.2021.00046.f4

potassium-containing particles, which are widely associated with biomass burning (Duan et al., 2004; Li et al., 2017), contributed 14.3% and 8.6% to total $PM_{2.5}$, respectively. SiO_3 particles, which could be related to crustal material, contributed 8.3% to total $PM_{2.5}$. The remaining species contributing to the chemical profile were EC and OC combined particles (7.0%), heavy metal particles (2.8%), high molecular OC particles (0.8%), sodium particles (0.2%), and others (0.08%). It should be noted that secondary species such as sulfate, nitrate, and ammonium are not present in the results since these ions have lower priority compared to EC and OC as per the ART-2a algorithm. For example, a particle consisting of both sulfate and EC will be classified as an EC-containing particle based on ART-2a. The spectra for the different types of particles are shown in Figure S4. It can be seen that sulfate and nitrate ions are present in almost all particle types with strong signals. However, the signal of NH_4^+ is relatively weak because the instrument is sensitive to alkali metal ions (especially K^+) but not for NH_4^+ (Liu et al., 2016). Overall, $PM_{2.5}$ from both mass and particle number concentrations indicated large contributions from carbon containing particles and secondary inorganic species, which is typical of urban $PM_{2.5}$ in China (e.g., Zhengzhou, Xi'an, Jinan, Chengdu, Chongqing, and Changsha; Tao et al., 2017).

3.2. Source identification

Source contributions of both particle mass and number concentration of $PM_{2.5}$ were apportioned by applying the PMF5.0 receptor model. The identification of sources was based on chemical tracers that are generally presumed to be emitted by specific sources and are present in significant amounts in the collected samples. **Figures 5** and **6** show profiles of the six identified sources from the PMF model based on particle mass and number concentration, respectively. We separately discuss each of the sources below.

3.2.1. Fossil fuel combustion

This source profile derived from $PM_{2.5}$ mass concentration (**Figure 5**) was characterized by high levels of Zn (74%), Fe (80%), Mn (48%), Pb (40%), Cd (21%), and V (18%), suggesting that it might represent fossil fuel combustion. This is supported by previous studies, which reported that sources traced by V were frequently interpreted as residual/fuel oil combustion from industrial processes, such as power plants and/or oil refineries, and the presence of Pb and Zn indicates anthropogenic fossil fuel combustion (Al-Momani, 2003; Hu and Balasubramanian, 2003; Song and Gao, 2009; Cong et al., 2010; Cheng et al., 2011). Additionally, OC (12%) and EC (16%) were present in this factor, consistent with the profile of emissions from coal combustion reported by Duan et al. (2006).

Adopting similar criteria as the mass concentration profile, the presence of relatively high levels of Ni (29%), Zn (29%), EC (28%), and OC (18%) in the particle number concentration profile also suggested dominance of fossil fuel combustion (**Figure 6**). This source assignment was further confirmed by the presence of polycyclic aromatic hydrocarbons (PAHs) in this factor. Previous studies have reported that particulate matters from combustion sources, especially coal combustion, contained significant amounts of PAHs (Su et al., 2004; Ravindra et al., 2006; Shen et al., 2013). The presence of sulphate, ammonium, and nitrate in this source suggested that these fossil fuel combustion particles might have been aged. Also, the presence of a few trace metals (Mo, Ag, Ge, and La) in this factor could indicate combustion or sulfur fumigation where fossil fuel is used.

3.2.2. Dust (crustal material)

The second factor showed abundance of Ca (66%), Ti (41%), Al (36%), and Mg (24%), which clearly indicated

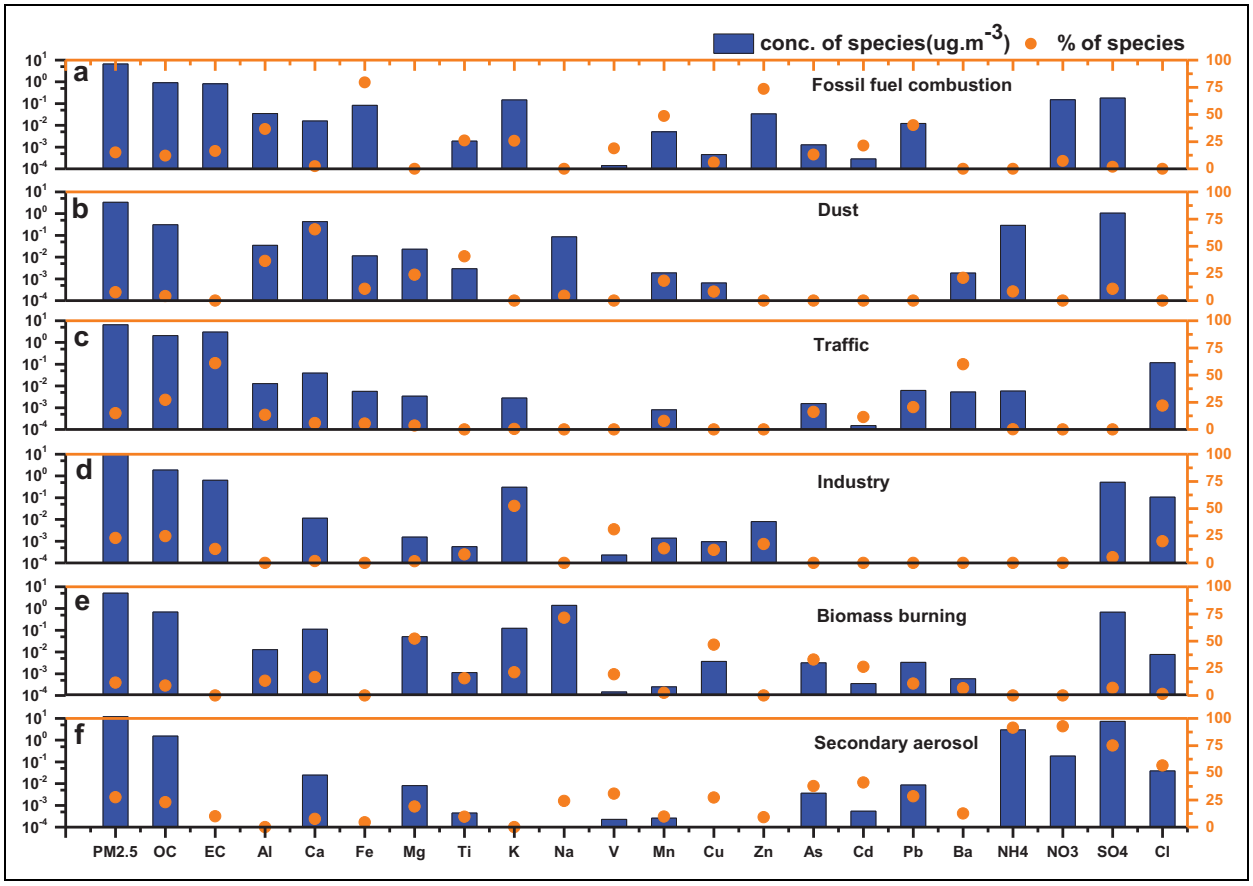

Figure 5. Profiles of six sources resolved using the PMF model based on chemical mass concentration, including fossil fuel combustion (a), soil dust (b), traffic (c), industrial emission (d), biomass burning (e), and secondary inorganic aerosol (f). Concentrations (μg m^{-3}) are shown on the left *Y*-axis and percentage of each species apportioned in the factors (circles) on the right *Y*-axis. DOI: https://doi.org/10.1525/elementa.2021.00046.f5

a dust source (**Figure 5**). Generally, high loadings of Ca, Al, Fe, Ti, and Sr are markers of crustal materials; especially, Ca, which is considered a tracer for construction dust, cement plants or lime kilns while Al and Ti represent crustal elements (Querol et al., 2002; Lucarelli et al., 2003; Almeida et al., 2005; Dall'Osto and Harrison, 2012). Interestingly, a much higher percentage of Ca (66%) compared to Al (36%) suggests Ca-rich dust in this source (Zhang et al., 2013). Similarly, based on single particle analysis, dust-related particles were characterized by high levels of Ca (55%), SiO_3^- (55%), Mg (38%), and Ti (23%; **Figure 6**), consistent with results from mass analysis. However, it is interesting to note that Pb containing particles (Pb, 66%) are also present in this source, possibly due to the presence of Pb oxidant in mineral dust (Langmann, 2013). Additionally, nitrate and sulfate signals appeared in this factor suggesting aging and evolution of mineral dust particles (Taiwo et al., 2014).

3.2.3. Traffic

EC is one of the most commonly used markers for vehicle emissions (Mao et al., 2018) while Ba, Zn, Pb, and Cu represent nonexhaust traffic sources such as motor vehicle lubricating oil, brake pad, or tire wear (Sternbeck et al., 2002; Thorpe and Harrison, 2008). Based on the source profiles of mass concentration, high levels of EC (61%) and Ba (60%; **Figure 5**) suggested this profile to be a traffic source. Other elements present in an appreciable amount in this source include Al (13%), Pb (20%), As (16%), and Mn (8%), which might be a signature of road traffic, especially from brake wear (Sternbeck et al., 2002; Thorpe and Harrison, 2008).

Based on particle number concentration, traffic emissions were characterized by high levels of SiO_3^- (55%), PO_3^- (41%), SO_4^{2-} (11%) and NO_3^- (13%; **Figure 6**). SiO_3^- and PO_3^- may indicate road dust that is correlated with vehicle activity (Zhang et al., 2013). As with the fossil fuel combustion and dust sources, nitrate and sulfate signals also appear in this factor possibly indicating aging and evolution of the particles. Interestingly, high levels of F, Cl, Br, Li, Mg, and Na are shown in this source, while untypical in traffic sources, may be a result of internal mixing of particles from multiples sources, and needs to be studied further.

3.2.4. Industry

Presence of high levels of Na (72%), Mg (52%), Cu (47%), As (33%), and Cd (26%) indicated that these particles could be from industrial emissions (**Figure 5**). Generally, glass manufacturing could generate a significant amount of Na and Mg-containing particles (Michelle, 1995), and it has been documented that glass production might

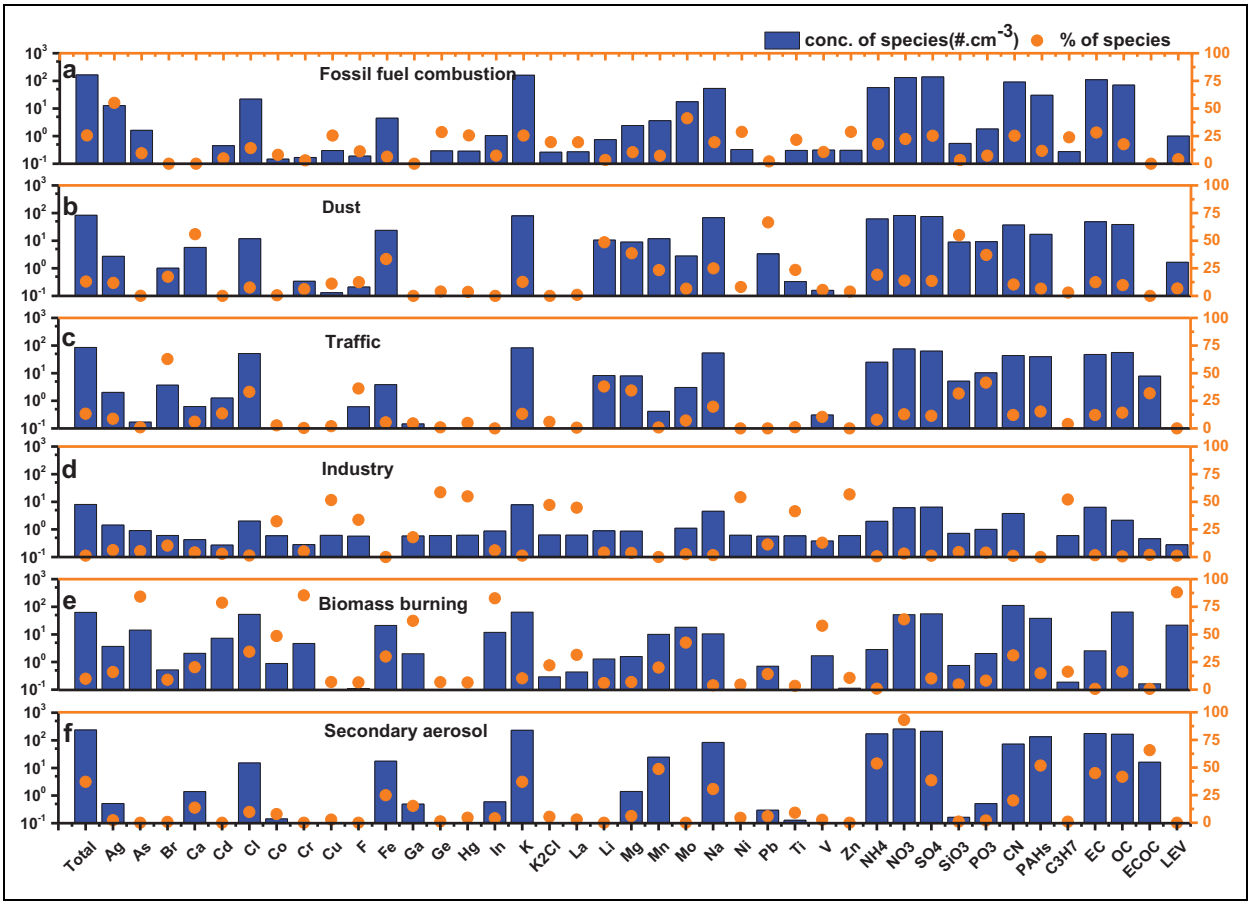

Figure 6. Profiles of six sources resolved using the PMF model based on chemical particle number concentration, including fossil fuel combustion (a), soil dust (b), traffic (c), industrial emission (d), biomass burning (e), and secondary inorganic aerosol (f). Concentrations (# cm^{-3}) are shown on the left *Y*-axis and percentage of each species apportioned in the factors (circles) on the right *Y*-axis. DOI: https://doi.org/10.1525/elementa.2021.00046.f6

contribute >20% of Na in $PM_{2.5}$ in Yulin city (based on local government report). Additionally, the presence of Cu and Cd in industrial emissions is supported by previous studies, which have reported emissions of Cu and As from Cu smelters and that of Cd from metallurgy (Alastuey et al., 2006; Querol et al., 2007). As for single particle analysis (**Figure 6**), the industrial emission source was characterized by high levels of Cu (52%). Other markers for this source included Co, Ni, Zn, Ti, La, Ge, Hg, and C_3H_7. La, Ga, and Co are believed to originate from sulfur-fumigation and ceramics processes (Swaine, 1994; Wang et al., 2003; Almeida et al., 2005; Xu et al., 2007).

3.2.5. Biomass burning

A high level of K (52%; **Figure 5**) represented the biomass burning factor, which has been reported in many source apportionment studies conducted in China (Cachier and Ducret, 1991; He et al., 2001; Watson et al., 2001; Zheng et al., 2005; He et al., 2006; Zhang et al., 2013). In the case of particle number concentration (**Figure 6**), biomass burning emissions were characterized by high levels of levoglucosan (53%), which is one of the most commonly used markers for biomass burning (He et al., 2006). Similarly, nitrate and sulfate signals also appeared in this factor indicating aging and evolution of these particles.

3.2.6. Secondary aerosol

Substantially high NO_3^- (93%), NH_4^+ (91%), and SO_4^{2-} (75%) were observed in the sixth factor as shown in **Figure 5**, which is the typical signature of secondary inorganic aerosol (Giorio et al., 2012). Interestingly, Cl and Na were also found in this source, which could indicate that sea-salt particles could have been present with a coating of ammonium sulfate on the surface (Ottley and Harrison, 1992). The source profile for number concentration concurs with that of mass concentration for this factor (**Figure 6**), showing strong signals of NH_4^+, SO_4^{2-}, and NO_3^-. Interestingly, large fractions of OC and EC-containing particles were also present in this source, which points to the possibility of agglomeration of EC and primary/aged OC with the secondary particles (Lin et al., 2017).

3.3. Comparison of source contributions

The comparison of source contributions based on mass concentration and number concentration is shown in **Figure 7.** In general, a relatively good agreement is observed for secondary species, traffic, and dust sources, but significant differences exist for industrial emission, fossil fuel combustion, and biomass burning. Although secondary compounds had the largest contribution to $PM_{2.5}$ based on both approaches (31% and 35%,

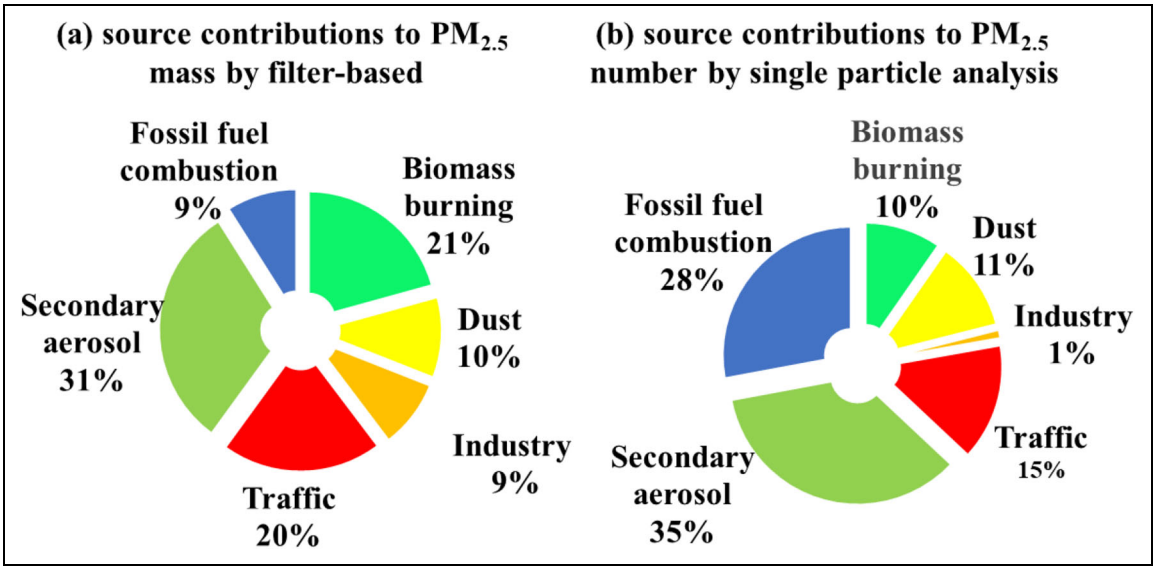

Figure 7. Comparison of source contributions to $PM_{2.5}$ during the study period based on (a) mass concentration and (b) number concentration. DOI: https://doi.org/10.1525/elementa.2021.00046.f7

respectively), the contribution by fossil fuel combustion had the largest difference between these two approaches (9% based on mass concentration against 28% based on number concentration). Additionally, the contribution of biomass burning to $PM_{2.5}$ based on mass concentration (21%) was much larger than that based on number concentration (9%). Industrial emissions have little contribution (only 1%) based on particle number concentration, while they showed much higher contribution (9%) based on particle mass concentration.

Given that the source contributions were obtained using two different techniques, it is difficult to explain why the methods can accurately predict the contribution of some sources while diverging in their prediction of other sources. The possible reasons for the difference in the source contribution from mass concentration and number concentration may include the following: (1) For particle mass concentration analysis, all compositions were quantified based on their mass. However, for particle number concentration analysis, particles were counted based only on the detectable signal while ignoring information on signal intensity. Therefore, the resultant fraction of elements in each source could be different. Although a scaling approach has been built to quantify mass concentration of chemical species based on analysis using SPAMS (Zhou et al., 2016), this approach was not adopted in the current study due to the lack of necessary data such as total particle number concentration measured using scanning mobility particle sizer spectrometer (SMPS); (2) the source analysis based on particle mass concentration does not consider the size effect whereas SPAMS differentiated the particles based on size prior to chemical characterization; (3) the measurement based on the mass concentration covered all $PM_{2.5}$ particles, while SPAMS only analyzed the particles larger than 200 nm; (4) single particle analysis may provide clues on the processing mechanism of particle formation while mass concentration is unable to do so. For example, more EC-containing particles were identified in the secondary source since EC could be coated with secondary species. For particle mass concentration, on the other hand, the degree of mixing between EC and secondary species could not be differentiated and considered; (5) different tracers with varying applicability have been used to identify the same source. For example, the biomass burning tracer used in single particle analysis (levoglucosan) is considered to be more robust than that used in mass concentration (K^+), since K^+ could be emitted from other sources such as dust, meat cooking, and steelworks sinter plant (Watson and Chow, 2001; Tsai et al., 2007; Dall'Osto et al., 2013; Hleis et al., 2013). Given the discrepancy between SPAMS and filter-based analysis, more comparative studies should be conducted at various locations and across seasons before standalone SPAMS data can be used with confidence. As the first study to compare these two approaches, our scope is limited to identifying the presence of discrepancies and speculating on the possible reasons. More research is needed before specific suggestions and guidelines on how to use single particle data, or general adjustment factors to enable comparison can be provided.

3.4. Diurnal variation and special case analysis

One of the advantages of source apportionment based on SPAMS is the higher time resolution, which enables us to analyze diurnal variations of source contributions and to study specific transient events.

3.4.1. Diurnal variation

Figure 8 shows the diurnal variation of different sources based on particle number concentration. Traffic emissions exhibited a peak between approximately 8:00 and 11:00 due to the morning rush hour and another peak between approximately 22:00 and 2:00 of the next day, which

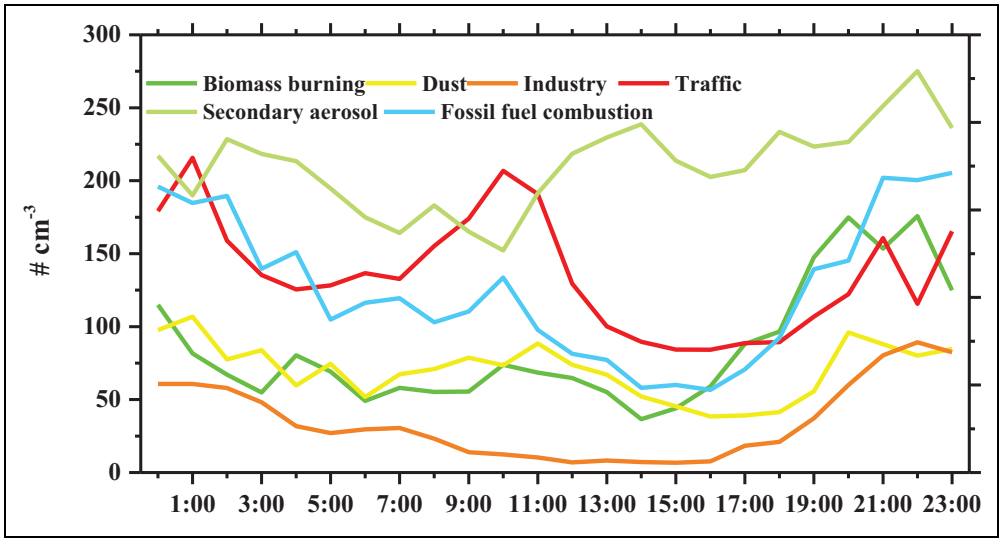

Figure 8. Diurnal variation of source contributions to $PM_{2.5}$ based on particle number concentration. DOI: https://doi.org/10.1525/elementa.2021.00046.f8

could be due to an increase in diesel vehicles during this time. According to the local government policy, diesel vehicles are prohibited from driving in the city until 22:00. The dust source showed stable contributions throughout the 24-h period. Biomass burning contributions were obviously increased during nighttime from about 19:00–22:00, which could be due to the influence of local cooking emissions during dinner time from restaurants near our monitoring site.

On the other hand, industrial emission and fossil fuel combustion showed higher concentrations during nighttime and lower during daytime, which might be because of a decrease in mixing height during nighttime along with a relatively constant emission strength (Li et al., 2015). The first peak of secondary compounds appeared at about 12:00–14:00, which is expected due to the increase in solar radiation and subsequent enhancement in photochemical reactions that promote the formation of secondary particles. However, in the evening, decrease in temperatures created inversion conditions that potentially accelerated the accumulation of atmospheric particulate matter. Therefore, the concentration of secondary compounds did not decrease significantly even with lower amounts of solar radiation. Furthermore, the peak of secondary compounds at about 2 AM could be due to nighttime nitrate chemistry in the form of nighttime oxidation and condensation of locally emitted NO_x that could have led to an increase in secondary aerosol formation (Brown et al., 2012; Rollins and Science, 2012; Edwards et al., 2017).

3.4.2. Special case analysis

One of the major advantages of the high time resolution of SPAMS measurements is that transient pollution events (spanning several hours) can be extracted and investigated. Two interesting cases with sudden increases in particle number concentration are demonstrated as follows (Figure S5), which went undetected in the filter-based particle mass concentration analysis. Case-I was recorded from February 29 21:00 to March 1 4:00 lasting for approximately 8 h. During this episode, secondary compounds were the major source of $PM_{2.5}$ accounting for 57% followed by the transportation at 19% (shown in **Figure 9a**). Biomass burning and dust particles accounted for 15% and 9%, respectively, while industrial and fossil fuel combustion sources were hardly present. Case-II was observed from March 17 18:00 to March 18 1:00 (approximately 8 h). In this case, the major source was from vehicle emissions, which accounted for 40% of the $PM_{2.5}$ particles followed by the secondary compounds (29%; shown in **Figure 9b**), while contributions from fossil fuel combustion and dust were 15% and 12%, respectively.

Case-I happened during the Chinese New Year period, one of most important Chinese festivals which is celebrated with intensive use of fireworks all over the country, both in megacities and in rural areas. Large amounts of SO_2 and VOCs—the precursors of secondary inorganic and organic compounds—could be emitted from fireworks causing a significant increase in the secondary compounds (Ciarelli et al., 2019). The increase of biomass burning particles (from 61 ± 98 # cm^{-3} to 567 # cm^{-3}, **Table 1**) during this period also confirmed the emission from fireworks. However, in Case-II, the particles from transportation increased the most (from 109 ± 158 # cm^{-3} to 885 ± 297 # cm^{-3}, **Table 1**). This could be due to an increase in diesel vehicles during nighttime on that date since diesel vehicles were only allowed to enter the urban area of Yulin city based on the policy of the local government. Additionally, particles due to secondary formation were increased from 259 ± 335 # cm^{-3} to 624 ± 163 # cm^{-3} (**Table 1**), which was potentially due to greater emissions of precursors of secondary species (e.g., NO_x (NO_2 + NO) and VOCs). The weather conditions were less favorable for pollutant accumulation in this case than for Case-I with lower wind speeds (Case-I wind speed: 0.4 m s^{-1}; Case-II wind speed: 0.8 m s^{-1}), which was further confirmed by longer backward trajectories from the southwest (Figure S6).

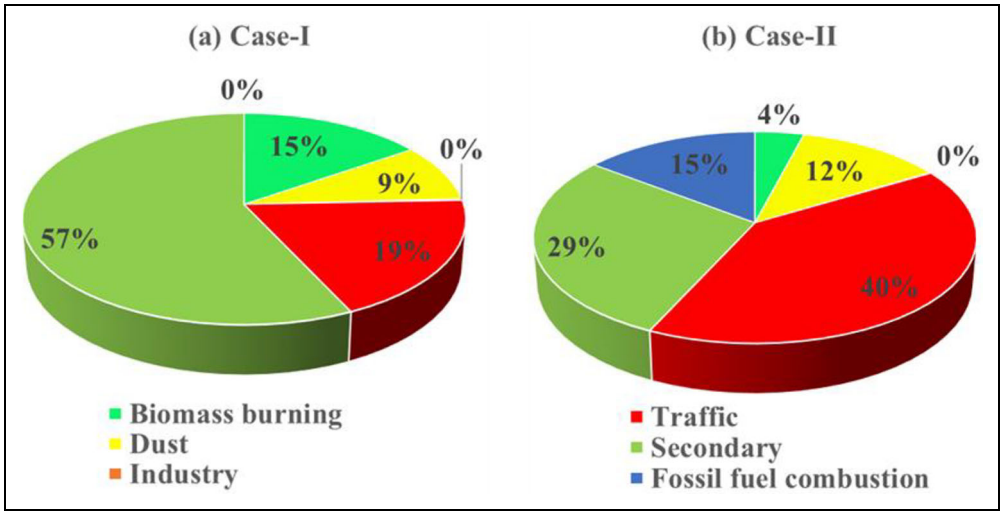

Figure 9. Source contributions to $PM_{2.5}$ based on particle number concentration for Case-I and Case II. DOI: https://doi.org/10.1525/elementa.2021.00046.f9

Table 1. $PM_{2.5}$ number concentration (# cm^{-3}) for six sources identified by positive matrix factorization during the two cases. DOI: https://doi.org/10.1525/elementa.2021.00046.t1

Case	Biomass Burning	Dust	Industry	Transportation	Secondary	Fossil Fuel Combustion	Subtotal
Case-I ($n = 8$) [a]	567 ± 148	324 ± 205	8 ± 4	688 ± 219	2104 ± 355	0	3692
Case-II ($n = 11$) [a]	89 ± 33	267 ± 138	3 ± 3	885 ± 297	624 ± 163	320 ± 119	4216
Average	61 ± 98	84 ± 99	8 ± 3	109 ± 158	259 ± 335	201 ± 140	693 ± 572

The data are presented as average ± standard deviations.

[a]The numbers in parentheses show the sample size (hourly).

4. Conclusions

This comparative study on aerosol source apportionment based on number and mass concentrations has demonstrated the advantages of SPAMS in terms of its capabilities to characterize aerosols at a single particle level, and specifically, its usefulness to investigate diurnal variations and episodic events, which are difficult to capture using the traditional filter-based approach. Overall, for mass concentration, the averaged $PM_{2.5}$ concentration for the entire measurement period was 42 ± 16 μg m^{-3} with sulfate (23.5%) and carbonaceous compounds (18.1%) dominating, while for particle number concentration, EC-containing particles had the largest contribution to $PM_{2.5}$ (42.2%), followed by OC-containing particles (15.7%). Source apportionment results showed that the six sources identified based on each of the two approaches were similar in general; however, differences were noted for industrial emission, fossil fuel combustion, and biomass burning, presumably due to differences in measurement techniques and/or marker ions. Two episodic events: one with enhanced firework activity during the Chinese New Year and another with increased diesel-related traffic emissions were analyzed to demonstrate the advantage of SPAMS analysis. In summary, single particle analysis can provide source apportionment with a high time resolution, which is helpful for the government to analyze and implement control strategies on an emergency basis for air pollution episodes. However, caution should be exercised while comparing SPAMS data with results generated based on the traditional filter-based approach, especially in terms of quantitative contributions of each source to ambient $PM_{2.5}$. We therefore suggest that SPAMS might be useful for the analysis of short-time air pollution episodes; however, for long-term source apportionment of air pollution, the traditional filter-based analysis should be relied upon, at least until the specific differences between these two approaches are robustly understood and quantified.

Data accessibility statement

Data summaries are provided in the supplemental materials.

Supplemental files

The supplemental files for this article can be found as follows:

Text S1–2, Figures S1–6, Tables S1–3.docx
Data S1.xlsx

Funding

This work has been funded by the National Key Research and Development Plan (2017YFC0210105), the National Natural Science Foundation of China (41905107, 41905086, and 41905105), Fundamental Research Funds for the Central Universities of China (20lgpy22), the China Postdoctoral Science Foundation (2020M683174), Guangdong Province Key Laboratory for Climate Change and Natural Disaster Studies (2020B1212060025), Special Fund Project for Science and Technology Innovation Strategy of Guangdong Province (2019B121205004), and the Jiangsu Collaborative Innovation Center for Climate Change.

Competing interests

The authors have no competing interests to declare.

Author contributions

Conceptualization, methodology, software, and writing: JM.

Visualization and investigation: YL.

Data curation and resources: ZM.

Supervision, writing- Original draft preparation: ZJ.

Investigation: KP, SS.

Visualization: QZ.

Methodology: WC, BZ.

Project administration, reviewing, and editing: SJ.

Project administration and funding acquisition: XW.

Interpreted the data and wrote the manuscript: YY.

All the authors commented and participated in the revision of the paper.

References

Al-Momani, IF. 2003. Trace elements in atmospheric precipitation at Northern Jordan measured by ICP-MS: Acidity and possible sources. *Atmospheric Environment* **37**: 4507–4515.

Alastuey, A, Querol, X, Plana, F, Viana, M, Ruiz, CR, Campa, ASDL, Rosa, JDL, Mantilla, E, Santos, SGD. 2006. Identification and chemical characterization of industrial particulate matter sources in southwest Spain. *Journal of the Air and Waste Management Association* **56**: 993–1006.

Allen, JO. 2001. Software Toolkit to Analyze Single-Particle Mass Spectral Data. Available at http://www.yaada.org.

Almeida, SM, Pio, CA, Freitas, MC, Reis, MA, Environment, MAT. 2005. Source apportionment of fine and coarse particulate matter in a sub-urban area at the Western European Coast. *Atmospheric Environment* **39**: 3127–3138.

Atkinson, RW, Fuller, GW, Anderson, HR, Harrison, RM, Armstrong, B. 2010. Urban ambient particle metrics and health: A time-series analysis. *Epidemiology* **21**: 501–511.

Bai, R, Lam, JCK, Li, VOK. 2018. A review on health cost accounting of air pollution in China. *Environment International* **120**: 279–294.

Baldauf, R, Thoma, E, Hay, M, Shores, R, Kinsey, J, Gullett, B, Kimbrough, S, Isakov, V, Long, T, Snow, R. 2002. $PM_{2.5}$ carbonate concentrations at regionally representative interagency monitoring of protected visual environment sites. *Journal of Geophysical Research: Atmospheres* **107**: D21.

Brems, D, Degryse, P. 2014. Trace element analysis in provenancing Roman glass-making. *Archaeometry* **56**: 116–136.

Brown, SS, Dubé, WP, Karamchandani, P, Yarwood, G, Peischl, J, Ryerson, TB, Neuman, JA, Nowak, JB, Holloway, JS, Washenfelder, RA. 2012. Effects of NO_x control and plume mixing on nighttime chemical processing of plumes from coal-fired power plants. *Journal of Geophysical Research: Atmospheres.***117**: 134–142.

Cachier, H, Ducret, J. 1991. Influence of biomass burning on equatorial African rains. *Nature* **352**: 228–230.

Chen, Y, Yang, F, Mi, T, Cao, J, Shi, G, Huang, R, Wang, H, Chen, J, Lou, S, Wang, Q. 2017. Characterizing the composition and evolution of and urban particles in Chongqing (China) during summertime. *Atmospheric Research* **187**: 84–94.

Cheng, K, Tian, H, Zhao, D, Lu, L, Wang, Y, Chen, J, Liu, X, Jia, W, Huang, Z. 2014. Atmospheric emission inventory of cadmium from anthropogenic sources. *International Journal of Environmental Science and Technology* **11**: 605–616.

Cheng, I, Xu, X, Zhang, L. 2015. Overview of receptor-based source apportionment studies for speciated atmospheric mercury. *Atmospheric Chemistry and Physics* **15**: 7877–7895.

Cheng, M, You, C, Lin, F, Huang, K, Chung, C. 2011. Sources of Cu, Zn, Cd and Pb in rainwater at a subtropical islet offshore northern Taiwan. *Atmospheric Environment* **45**: 1919–1928.

Chow, JC, Watson, JG, Pritchett, LC, Pierson, WR, Frazier, CA, Purcell, RG. 1993. The dri thermal/optical reflectance carbon analysis system: Description, evaluation and applications in U.S. Air quality studies. *Atmospheric Environment. Part A. General Topics* **27**: 1185–1201.

Ciarelli, G, Theobald, MR, Vivanco, MG, Beekmann, M, Aas, W, Andersson, C, Bergström, R, Manders-Groot, A, Couvidat, F, Mircea, M, Tsyro, S, Fagerli, H, Mar, K, Raffort, V, Roustan, Y, Pay, MT, Schaap, M, Kranenburg, R, Adani, M, Briganti, G, Cappelletti, A, D'Isidoro, M, Cuvelier, C, Cholakian, A, Bessagnet, B, Wind, P, Colette, A. 2019. Trends of inorganic and organic aerosols and precursor gases in Europe: Insights from the EURODELTA multi-model experiment over the 1990–2010 period. *Geoscientific Model Development* **12**: 4923–4954.

Cong, Z, Kang, S, Zhang, Y, Li, X. 2010. Atmospheric wet deposition of trace elements to central Tibetan Plateau. *Applied Geochemistry* **25**: 1415–1421.

Dall'Osto, M, Harrison, RM. 2012. Urban organic aerosols measured by single particle mass spectrometry in the megacity of London. *Atmospheric Chemistry and Physics* **12**: 4127–4142.

Dall'Osto, M, Querol, X, Amato, F, Karanasiou, A, Lucarelli, F, Nava, S, Calzolai, G, Chiari, M. 2013.

Hourly elemental concentrations in $PM_{2.5}$ aerosols sampled simultaneously at urban background and road site during SAPUSS – Diurnal variations and PMF receptor modelling. *Atmospheric Chemistry and Physics* **13**: 4375–4392.

DeCarlo, PF, Kimmel, JR., Trimborn, A, Northway, MJ, Jayne, JT, Aiken, AC, Gonin, M, Fuhrer, K, Horvath, T, Docherty, KS, Worsnop, DR, Jimenez, JL. 2006. Field-deployable, high-resolution, time-of-flight Aerosol Mass Spectrometer. *Analytical Chemistry* **78**: 8281–8289.

Duan, F, Liu, X, Yu, T, Cachier, H. 2004. Identification and estimate of biomass burning contribution to the urban aerosol organic carbon concentrations in Beijing. *Atmospheric Environment* **38**: 1275–1282.

Duan, F, He, K, Ma, Y, Yang, F, Yu, X, Cadle, S, Chan, T, Mulawa, PA. 2006. Concentration and chemical characteristics of $PM_{2.5}$ in Beijing, China: 2001–2002. *Science of the Total Environment* **355**: 264–275.

Edwards, PC, Aikin, K, Dubé, WL, Fry, J, Gilman, J, de Gouw, J, Graus, M, Hanisco, T, Holloway, J, Hübler, G, Kaiser, JN, Keutsch, F, Lerner, BA, Neuman, J, Parrish, D, Peischl, J, Pollack, I, Ravishankara, AR, Roberts, J, Brown, S. 2017. Transition from high- to low-NOx control of nighttime oxidation in the southeastern US. *Nature Geoscience* **10**(7): 490–495.

European Environment Agency. 2015. Air quality in Europe, 2014. Available at http://www.eea.europa.eu/publications/air-quality-in-europe-2014. Accessed 21 September 2015.

Figueroa, DA, Rodríguez-Sierra, CJ, Jiménez-Velez, BD. 2006. Concentrations of Ni and V, other heavy metals, arsenic, elemental and organic carbon in atmospheric fine particles ($PM_{2.5}$) from Puerto Rico. *Toxicology and industrial health* **22**: 87–99.

Gao, J, Wang, J, Cheng, SH, Xue, LK, Yan, HZ, Hou, LJ, Jiang, YQ, Wang, WX. 2007. Number concentration and size distributions of submicron particles in Jinan urban area: Characteristics in summer and winter. *Journal of Environmental Sciences* **19**: 1466–1473.

Gao, J, Wang, T, Zhou, X, Wu, W, Wang, W. 2009. Measurement of aerosol number size distributions in the Yangtze River delta in China: Formation and growth of particles under polluted conditions. *Atmospheric Environment* **43**: 829–836.

Giorio, C, Tapparo, A, Dall'Osto, M, Harrison, RM, Beddows, DCS, Marco, CD, Nemitz, E. 2012. Comparison of three techniques for analysis of data from an Aerosol Time-of-Flight Mass Spectrometer. *Atmospheric Environmen* **61**: 316–326.

Gross, DS, Galli, ME, Silva, PJ, Prather, K. 2000. Relative sensitivity factors for alkali metal and ammonium cations in single-particle aerosol time-of-flight mass spectra chem. *Environmental Science & Technology* **72**: 416–422.

Guo, S, Hu, M, Wang, ZB, Slanina, J, Zhao, YL. 2010. Size-resolved aerosol water-soluble ionic compositions in the summer of Beijing: Implication of regional secondary formation. *Atmospheric Chemistry and Physics* **10**: 947–959.

He, K, Yang, F, Ma, Y, Zhang, Q, Yao, X, Chan, CK, Cadle, S, Chan, T, Mulawa, P. 2001. The characteristics of $PM_{2.5}$ in Beijing, China. *Atmospheric Environmen* **35**: 4959–4970.

He, L, Hu, M, Huang, X, Zhang, Y, Tang, X. 2006. Seasonal pollution characteristics of organic compounds in atmospheric fine particles in Beijing. *Science of the Total Environment* **359**: 167–176.

Hleis, D, Fernández-Olmo, I, Ledoux, F, Kfoury, A, Courcot, L, Desmonts, T, Courcot, D. 2013. Chemical profile identification of fugitive and confined particle emissions from an integrated iron and steelmaking plant. *Journal of hazardous materials* **250**: 246–255.

Hu, GP, Balasubramanian, R. 2003. Wet deposition of trace metals in Singapore. *Water, Air, and Soil Pollution* **144**: 285–300.

Huang, X, He, L, Hu, M, Canagaratna, MR, Sun, Y, Zhang, Q, Zhu, T, Xue, L, Zeng, L, Liu, X, Zhang, Y, Jayne, JT, Ng, NL, Worsnop, DR. 2010. Highly time-resolved chemical characterization of atmospheric submicron particles during 2008 Beijing Olympic Games using an Aerodyne High-Resolution Aerosol Mass Spectrometer. *Atmospheric Chemistry and Physics* **10**: 8933–8945.

Huang, XHH, Bian, Q, Ng, W, Louie, P, Yu, J. 2014. Characterization of $PM_{2.5}$ major components and source investigation in suburban Hong Kong: A one year monitoring study. *Aerosol and Air Quality Research* **14**: 235–250.

Huang X, Yun H, Gong Z, Li X, He L, Zhang Y, Hu M. 2014.Air pollution characteristic and variation trend of Central Triangle urban agglomeration from 2005 to 2014. *Chinese Journal of Environmental Engineering* **44**: 723–734.

Jayne, JT, Leard, DC, Zhang, X, Davidovits, P, Smith, KA, Kolb, CE, Worsnop, DR. 2000. Development of an Aerosol Mass Spectrometer for Size and Composition Analysis of Submicron Particles. *Aerosol Science and Technology* **33**: 49–70.

Kelly, KE, Sarofim, AF, Lighty, JS. 2003. *User guide for characterizing particulate matter: Evaluation of several real-time methods*. Available at https://apps.dtic.mil/sti/citations/ADA462282.

Kochy, F, Chow, JC, Watson, JG. 2002. Evaluation of OC/EC speciation by thermal manganese dioxide oxidation and the IMPROVE method. *Journal of the Air & Waste Management Association* **52**: 1333–1341.

Langmann, B. 2013. Volcanic ash versus mineral dust: Atmospheric processing and environmental and climate impacts. *ISRN Atmospheric Science*s **2013**: 1–17.

Li, J, Xu, T, Lu, X, Chen, H, Nizkorodov, SA, Chen, J, Yang, X, Mo, Z, Chen, Z, Liu, H, Mao, J, Liang, G. 2017. Online single particle measurement of

fireworks pollution during Chinese New Year in Nanning. *Journal of Environmental Sciences* **53**: 184–195.

Li, L, Huang, Z, Dong, J, Li, M, Gao, W, Nian, H, Fu, Z, Zhang, G, Bi, X, Cheng, P, Zhou Z. 2011. Real time bipolar time-of-flight mass spectrometer for analyzing single aerosol particles. *International Journal of Mass Spectrometry* **303**: 118–124.

Li, M, Tang, G, Huang, J, Liu, Z, An, J, Wang, Y. 2015. Characteristics of winter atmospheric mixing layer height in Beijing-Tianjin-Hebei region and their relationship with the atmospheric pollution. *Enviromental Science* **36**(06): 1935–1943.

Lin, Q, Zhang, G, Peng, L, Bi, X, Wang, X, Brechtel, FJ, Li, M, Chen, D, Peng, PA, Sheng, G, Zhou, Z. 2017. In situ chemical composition measurement of individual cloud residue particles at a mountain site, southern China. *Atmospheric Chemistry and Physics* **17**: 1–39.

Liu, S, Hu, M, Wu, Z, Wehner, B, Wiedensohler, A, Cheng, Y. 2008. Aerosol number size distribution and new particle formation at a rural/coastal site in Pearl River Delta (PRD) of China. *Atmospheric Environment* **42**: 6275–6283.

Lucarelli, A, Lupi, S, Ortolani, M, Calvani, P, Maselli, P, Capizzi, M, Giura, P, Eisaki, H, Kikugawa, N, Fujita, T. 2003. Phase diagram of La_2-x$SrxCuO_4$ probed in the infared: imprints of charge stripe excitations. *Physical Review Letters* **90**: 259–294.

Ma, L, Li, M, Zhang, H, Li, L, Huang, Z, Gao, W, Chen, D, Fu, Z, Nian, H, Zou, L, Gao, J, Chai, F, Zhou, Z. 2016. Comparative analysis of chemical composition and sources of aerosol particles in urban Beijing during clear, hazy, and dusty days using single particle aerosol mass spectrometry. *Journal of Cleaner Production* **112**: 1319–1329.

Mao, J, Chen, Z, Mo, Z, Yang, X, Li, H, Liu, Y, Liu, H, Huang, J, Yang, J, Li, H. 2018. Highly time-resolved aerosol characteristics during springtime in Weizhou Island. *Journal of Environmental Sciences* **72**: 64–74.

Masiol, M, Harrison, RM, Vu, TV, Beddows, DCS. 2017. Sources of sub-micrometre particles near a major international airport. *Atmospheric Chemistry and Physics* **17**: 12379–12403.

Maji, KJ, Ye, W, Arora, M, Shiva Nagendra, SM. 2018. $PM_{2.5}$-related health and economic loss assessment for 338 Chinese cities. *Environment International* **121**: 392–403.

Mazzei, F, D'Alessandro, A, Lucarelli, F, Nava, S, Prati, P, Valli, G, Vecchi, R. 2008. Characterization of particulate matter sources in an urban environment. *Science of the Total Environment* **401**: 81–89.

Michelle, M. 1995. *Ambient air and stationary source emission - Determination of metals in ambient particulate matter - Inductively couple plasma/mass spectrometry (ICP-MS).* HJ 657–2013. ASM International. Handbook Committee. Technology & Engineering Ministry of Environmental Protection, 2013.

Ministry of Ecology and Environment of the People's Republic of China. 2015. Ambient air and waste gas from stationary sources emission - Determination of metal elements in ambient particle matter - Inductively coupled plasma optical emission spectrometry (HJ777-2015). Available at 2015. https://www.mee.gov.cn/ywgz/fgbz/bz/bzwb/jcffbz/201512/t20151214_319107.shtml.

Ottley, CJ, Harrison, RM. 1992. The spatial distribution and particle size of some inorganic nitrogen, sulphur and chlorine species over the North Sea. *Atmospheric Environment Part A: General Topics* **26**: 1689–1699.

Pandolfi, M, Gonzalez-Castanedo, Y, Alastuey, A, de la Rosa, JD, Mantilla, E, de la Campa, AS, Querol, X, Pey, J, Amato, F, Moreno, T. 2011. Source apportionment of PM_{10} and $PM_{2.5}$ at multiple sites in the strait of Gibraltar by PMF: Impact of shipping emissions. *Environmental Science and Pollution Research* **18**: 260–269.

Peter, A. Jaques, CS. 2000. Measurement of total lung deposition of inhaled ultrafine particles in healthy men and women. *Inhalation Toxicology* **12**: 715–731.

Prather, KA, Hatch, CD, Grassian, VH. 2008. Analysis of atmospheric aerosols, annual review of analytical chemistry. *Annual Reviews of Analytical Chemistry* **1**: 485–514.

Querol, X, Alastuey, A, Rosa, JDL, Sánchez-De-La-Campa, A, Plana, F, Ruiz, CR. 2002. Source apportionment analysis of atmospheric particulates in an industrialised urban site in southwestern Spain. *Atmospheric Environment* **36**: 3113–3125.

Querol, X, Viana, M, Alastuey, A, Amato, F, Moreno, T, Castillo, S, Pey, J, Rosa, JDL, Campa, ASDL, Artíñano, B. 2007. Source origin of trace elements in PM from regional background, urban and industrial sites of Spain. *Atmospheric Environment* **41**: 7219–7231.

Ravindra, K, Bencs, L, Wauters, E, Hoog, JD, Deutsch, F, Roekens, E, Bleux, N, Berghmans, P, Grieken, RV. 2006. Seasonal and site-specific variation in vapour and aerosol phase PAHs over Flanders (Belgium) and their relation with anthropogenic activities. *Atmospheric Environment* **40**: 771–785.

Rollins, AW, Browne, EC, Min, KE, Pusede SE, Wooldridge, PJ, Gentner, DR, Goldstein, AH, Liu, S, Day, DA, Russell, LM., Cohen, RC. 2012. Evidence for NO(x) control over nighttime SOA formation. *Science* **337**: 1210.

Salma, I, Füri, P, Németh, Z, Balásházy, I, Hofmann, W, Farkas, Á. 2015. Lung burden and deposition distribution of inhaled atmospheric urban ultrafine particles as the first step in their health risk assessment. *Atmospheric Environment* **104**: 39–49.

Seaton, A, Godden, D, MacNee, W, Donaldson, K. 1995. Particulate air pollution and acute health effects. *The Lancet* **345**: 176–178.

Shen, HZ, Huang, Y, Wang, R, Zhu, D, Li, W, Shen, GF, Wang, B, Zhang, YY, Chen, YC, Lu, Y, Chen, H, Li, TC, Sun, K, Li, BG, Liu, WX, Liu, JF, Tao, S. 2013. Global atmospheric emissions of polycyclic aromatic

hydrocarbons from 1960 to 2008 and future predictions. *Environmental Science & Technology* **47**(12): 6415–6424.

Shen, X, Sun, J, Zhang, Y, Wehner, B, Nowak, A, Tuch, T, Zhang, X, Wang, T, Zhou, H, Zhang, X, Dong, F, Birmili, W, Wiedensohler, A. 2011. First long-term study of particle number size distributions and new particle formation events of regional aerosol in the North China Plain. *Atmospheric Chemistry and Physics* **11**: 1565–1580.

Shen, H, Ye, H, Rong, W, Dan, Z, Li, WL, Shen, G, Bin, W, Zhang, Y, Chen, Y, Lu, Y, Chen, H, Li, T, Sun, K, Liu, W, Tao, S. 2013. Global atmospheric emissions of polycyclic aromatic hydrocarbons from 1960 to 2008 and future predictions. *Environmental Science & Technology* **47**: 6415–6424.

Shi, L, Zanobetti, A, Kloog, I, Coull, BA, Koutrakis, P, Melly, SJ, Schwartz, JD. 2016. Low-Concentration $PM_{2.5}$ and mortality: Estimating acute and chronic effects in a population-based study. *Environmental Health Perspectives* **124**: 46–52.

Smyth, AM, Thompson, SL, Foy, BD, Olson, MR, Sager, N, Mcginnis, J, Schauer, JJ, Gross, DS. 2013. Sources of metals and bromine-containing particles in Milwaukee. *Atmospheric Environment* **73**: 124–130.

Song, F, Gao, Y. 2009. Chemical characteristics of precipitation at metropolitan Newark in the US East Coast. *Atmospheric Environment* **43**: 4903–4913.

Song, Y, Xie, S, Zhang, Y, Zeng, L, Salmon, LG, Zheng, M. 2006. Source apportionment of $PM_{2.5}$ in Beijing using principal component analysis/absolute principal component scores and UNMIX. *Science of the Total Environment* **372**: 278–286.

Stanier, CO, Khlystov, AY, Pandis, SN. 2004. Ambient aerosol size distributions and number concentrations measured during the Pittsburgh Air Quality Study (PAQS). *Atmospheric Environment* **38**: 3275–3284.

Sternbeck, J, Sjödin, Å, Kenth, A. 2002. Metal emissions from road traffic and the influence of resuspension-results from two tunnel studies.*Atmospheric Environment* **36**: 4735–4744.

Su, G, Xu, X, Chow, JC, John, W, Sheng, Q, Liu, W, Bai, Z, Zhu, T, Zhang, J. 2004. Emissions of air pollutants from household stoves: Honeycomb coal versus coal cake. *Environmental Science & Technology* **38**: 4612.

Sun, Y, Wang, Z, Fu, P, Yang, T, Jiang, Q, Dong, H, Li, J, Jia, J. 2013. Aerosol composition, sources and processes during wintertime in Beijing, China. *Atmospheric Chemistry and Physics* **13**: 4577–4592.

Swaine, DJ. 1994. Trace elements in coal and their dispersal during combustion. *Fuel Processing Technology* **39**: 121–137.

State Council of PRC. 2013. State Council of PRC Air Pollution Prevention and Control Action Plan. Available at http://www.gov.cn/zwgk/2013-09/12/content_2486773.htm.

Taiwo, AM, Harrison, RM, Beddows, DCS, Shi, Z. 2014. Source apportionment of single particles sampled at the industrially polluted town of Port Talbot, United Kingdom by ATOFMS. *Atmospheric Environment* **97**: 155–165.

Tan, JH, Duan, JC, Chai, FH, He, KB, Hao, JM. 2014. Source apportionment of size segregated fine/ultrafine particle by PMF in Beijing. *Atmospheric Research* **139**: 90–100.

Tao, J, Cheng, T, Zhang, R. 2012. Chemical composition of summertime $PM_{2.5}$ and Its relationship to aerosol optical properties in Guangzhou, China. *Atmospheric and Oceanic Science Letters* **5**: 88–94.

Tao, J, Zhang, L, Cao, J, Zhang, R. 2017. A review of current knowledge concerning $PM_{2.5}$ chemical composition, aerosol optical properties and their relationships across China. *Atmospheric Chemistry and Physics* **17**: 9485–9518.

Thorpe, A, Harrison, RM. 2008. Sources and properties of non-exhaust particulate matter from road traffic: A review. *Science of the Total Environment* **400**: 270–282.

Tian, Y, Wang, J, Peng, X, Shi, G, Feng, Y. 2014. Estimation of the direct and indirect impacts of fireworks on the physicochemical characteristics of atmospheric PM_{10} and $PM_{2.5}$. *Atmospheric Chemistry and Physics* **14**: 9469–9479.

Tsai, J, Lin, K, Chen, C, Ding, J, Choa, CG, Chiang, H. 2007. Chemical constituents in particulate emissions from an integrated iron and steel facility. *Journal of Hazardous Materials* **147**: 111–119.

Ulbrich, IM, Canagaratna, MR, Zhang, Q, Worsnop, DR, Jimenez, JL. 2009. Interpretation of organic components from positive matrix factorization of aerosol mass spectrometric data. *Atmospheric Chemistry and Physics* **9**: 2891–2918.

Upadhyay, N, Clements, AL, Fraser, MP, Sundblom, M, Solomon, P, Herckes, P. 2015. Size-differentiated chemical composition of re-suspended soil dust from the Desert Southwest United States. *Aerosol and Air Quality Research* **15**: 387–398.

Wang, R, Pan, W, Chen, J, Jiang, M, Luo, Y. 2003. Properties and microstructure of machinable AlO/LaPO ceramic composites.*Ceramics Internationa* **29**: 19–25.

Wang, Z, Hu, M, Zeng, L, Xue, L, He, L, Huang, X, Zhu, T. 2014. Measurements of particle number size distributions and optical properties in urban Shanghai during 2010 World Expo: Relation to air mass history. *Tellus B: Chemical and Physical Meteorology* **66**: 22319.

Wang, X, Zhao, Q, Cui, H. 2015. PM2.5 source apportionment at suburb of Shanghai in winter based on real time monitoring. *Journal of Nanjing University (Natural Sciences)* **51**: 517–523.

Wang, S, He, B, Yuan, M, Su, F, Yin, S, Yan, Q, Jiang, N, Zhang, R, Tang, X. 2019. Characterization of individual particles and meteorological conditions during the cold season in Zhengzhou using a single particle aerosol mass spectrometer. *Atmospheric Research* **219**: 13–23.

Watson, JG, Chow, JC. 2001. Source characterization of major emission sources in the Imperial and Mexicali Valleys along the US/Mexico border. *Science of the Total Environment* **276**: 33–47.

Watson, JG, Chow, JC, Houck, JE. 2001. $PM_{2.5}$ chemical source profiles for vehicle exhaust, vegetative burning, geological material, and coal burning in Northwestern Colorado during 1995. *Chemosphere* **43**: 1141–1151.

Wise, J, Payne, R, Wise, S, Falank, C, Wise, J, Gianios, C, Douglas Thompson, W, Perkins, C, Zheng, T, Zhu, C, Benedict, L, Kerr, I. 2009. A global assessment of chromium pollution using sperm whales (Physeter macrocephalus) as an indicator species. *Chemosphere* **75**(11): 1461–1467. DOI: http://dx.doi.org/10.1016/j.chemosphere.2009.02.044.

Woo, KS, Chen, DR, Pui, DY, Mcmurry, PH. 2001. Measurement of Atlanta aerosol size distributions: Observations of ultrafine particle events. *Aerosol Science and Technology* **34**: 75–87.

World Health Organization. 2000. Air Quality Guidelines for Europe. European Series No 91. Geneva, Switzerland: World Health Organization. WHO Regional Publications.

World Health Organization. 2014. Burden of disease from air pollution. Available at http://www.who.int/phe/health_topics/outdoorair/databases/FINAL_HAP_AAP_BoD_24March2014.pdf. Accessed 12 May 2016.

Wu, C, Yu, J. 2016. Determination of primary combustion source organic carbon-to-elemental carbon (OC/EC) ratio using ambient OC and EC measurements: Secondary OC-EC correlation minimization method. *Atmospheric Chemistry and Physics* **16**: 5453–5465.

Xie, Y, Dai, H, Zhang, Y, Wu, Y, Hanaoka, T, Masui, T. 2019. Comparison of health and economic impacts of $PM_{2.5}$ and ozone pollution in China. *Environment International* **130**: 104881.

Xu, C, Wang, H, Yang, Y, Jiang, Q. 2007. Effect of Al–P–Ti–TiC–Nd_2O_3 modifier on the microstructure and mechanical properties of hypereutectic Al–20 wt. %Si alloy. *Materials Science and Engineering: A* **452**: 341–346.

Yet Another ATOFMS Data Analyzer. 2008. Available at http:// www.yaada.org.

Yue, D, Hu, M, Wu, Z, Wang, Z, Guo, S, Wehner, B, Nowak, A, Achtert, P, Wiedensohler, A, Jung, J. 2009. Characteristics of aerosol size distributions and new particle formation in the summer in Beijing. *Journal of Geophysical Research: Atmospheres* **114**: 1159–1171.

Zhang, G, Han, B, Bi, X, Dai, S, Huang, W, Chen, D, Wang, X, Sheng, G, Fu, J, Zhou, Z. 2015. Characteristics of individual particles in the atmosphere of Guangzhou by single particle mass spectrometry. *Atmospheric Research* **153**: 286–295.

Zhang, J, Huang, X, Wang, Y, Luo, B, Zhang, J, Song, H, Zhang, W, Liu, P, Schäfer, K, Wang, S, Luo, J, Wu, P. 2018. Characterization, mixing state, and evolution of single particles in a megacity of Sichuan Basin, southwest China. *Atmospheric Research* **209**: 179–187.

Zhang, R, Jing, J, Tao, J, Hsu, SC, Wang, G, Cao, J, Lee, CSL, Zhu, L, Chen, Z, Zhao, Y, Shen, Z. 2013. Chemical characterization and source apportionment of $PM_{2.5}$ in Beijing: seasonal perspective. *Atmospheric Chemistry and Physics* **13**: 7053–7074.

Zheng, X, Liu, X, Zhao, F, Duan, F, Tong, Y, Cachier, HJ. 2005. Seasonal characteristics of biomass burning contribution to Beijing aerosol. *Science China Chemistry* **48**: 481–488.

Zhou, Y, Huang, XHH, Griffith, SM, Li, M, Li, L, Zhou, Z, Wu, C, Meng, J, Chan, CK, Louie, PKK, Yu, JZ. 2016. A field measurement based scaling approach for quantification of major ions, organic carbon, and elemental carbon using a single particle aerosol mass spectrometer. *Atmospheric Environment* **143**: 300–312.

Zong, Z, Wang, X, Tian, C, Chen, Y, Qu, L, Ji, L, Zhi, G, Li, J, Zhang, G. 2016. Source apportionment of PM2.5 at a regional background site in North China using PMF linked with radiocarbon analysis: insight into the contribution of biomass burning. *Atmospheric Chemistry and Physics* **16**: 11249–11265.

How to cite this article: Mao, J, Yang, L, Mo, Z, Jiang, Z, Krishnan, P, Sarkar, S, Zhang, Q, Chen, W, Zhong, B, Yang, Y, Jia, S, Wang, X. 2021. Comparative study of chemical characterization and source apportionment of $PM_{2.5}$ in South China by filter-based and single particle analysis. *Elementa: Science of the Anthropocene* 9(1). DOI: https://doi.org/10.1525/elementa.2021.00046.

Domain Editor-in-Chief: Detlev Helmig, Boulder AIR LLC, Boulder, CO, USA

Associate Editor: Md Firoz Khan, Department of Chemistry, University of Malaya, Kuala Lumpur, Malaysia

Knowledge Domain: Atmospheric Science

Part of an Elementa Special Feature: Pan-Pacific Anthropocene

Published: April 5, 2021 **Accepted:** February 2, 2021 **Submitted:** May 1, 2020

ELEMENTA Science of the Anthropocene

Elem Sci Anth is a peer-reviewed open access journal published by University of California Press.

OPEN ACCESS